

Micromechanical estimation of hydro-mechanical parameters in unsaturated microcracked concrete

A. Tognevi

CEA Saclay, DEN/DPC/SCCME/LECBA

Ecole Normale Supérieure de Cachan, LMT

B. Bary

CEA Saclay, DEN/DPC/SCCME/LECBA

A. Delaplace

Ecole Normale Supérieure de Cachan, LMT

ABSTRACT: This paper deals with the influence of microcracking on the hydro-mechanical behavior of hardened cement paste in unsaturated conditions. We focus in particular on the effects of the spatial distribution (random and aligned) of microcracks on the Biot tensor. A multi-coated sphere assemblage model (Bary et al. 2005) for hcp involving the main hydrates, the porosity and the anhydrous is used to describe its microstructure. Both generalized self-consistent scheme and the explicit effective medium approximation scheme due to Zheng & Du (2001) are then applied to estimate the macroscopic parameters of the intact material. The initial porosity is represented by an appropriate pore distribution which permits to calculate the saturation degree as a function of the capillary pressure, and to take into account the disjoining pressure in the thin film adsorbed on the solid phase in the partially saturated pores. At the mesoscale, the induced microporosity is represented by penny-shaped ellipsoidal voids. The evolution of Biot tensor as a function of both saturation degree and microcrack density parameter is then studied and discussed.

1 INTRODUCTION

Durability of cement-based materials in civil engineering is a great challenge, especially in the case of interim storage concrete structures containing nuclear waste. Such structures can indeed be subjected at long term to thermal loadings inducing cracking. Cracks then accelerate transport phenomena through the structure and are a major degradation factor at the origin of performance loss. Concrete is a complex material with behavior depending on multi-physics processes. In the particular context of thermo-hydro-mechanical loading, one of the most important factors controlling the mechanical response is the Biot tensor, which evolution is well known to be ruled by the saturation degree in unsaturated conditions. Its identification requires expensive and complex experiments. Various micromechanical models are devoted to predict by means of effective medium schemes the macroscopic properties of concrete, but few address the problem of the Biot tensor in unsaturated conditions. We propose in this study, on the basis of a multi-coated sphere model involving the main components resulting from the hydration of cement, an estimation of the Biot tensor as a func-

tion of both saturation degree and microcracks density. It is well known that at low saturation degrees the liquid phase is present in the form of thin films adsorbed on the solid phase surface in those pores which are emptied of free water. This phenomenon induces mechanical forces due to disjoining pressure on the solid phase. Its effects will be investigated in this paper. For the modeling of the induced damage in concrete we choose to represent the microcracks by penny-shaped ellipsoids. Randomly distributed microcracks have been several times studied in the literature by means of different effective medium approximation schemes (Deudé et al. 2002). In this work we focus on realistic loading conditions where microcracks can have particular orientations and distributions such that the effective medium is transverse isotropic. The paper is organized as follows: Section 2 presents the micromechanical model proposed for the hydrated cement paste (hcp). A brief introduction of hcp microstructure is then presented. In section 3, estimations of the Biot coefficient of the sphere model coatings are made by means of the Interaction Direct Derivative (IDD) model. This permits to obtain the Biot tensor of the intact whole assembly in section 4. Finally in section 5 the influ-

ence of the spatial distribution of microcracks on the Biot tensor of hcp is examined.

2 MODELLING

Concrete is a multi-scale heterogeneous material. The characteristic sizes of the different phases composing hcp range from the nanometer to micrometer scales. A realistic homogenization model has to take into account the different phases resulting from the hydration of cement, their shapes, sizes, and spatial distributions. It is well known that the main hydration products in the case of CEM I cement are C-S-H, calcium hydroxide (CH), and aluminates phases (ettringite and monosulfoaluminate).

2.1 Hcp multi-coated sphere model

The complex microstructure of hcp necessitates a realistic homogenization model to estimate correctly its effective macroscopic properties. Various micromechanical models for hcp exist in the literature. Zimmerman (1986) firstly modeled hcp as two-phase composite consisting in a solid matrix weakened by spheroidal pores. On the basis of recent nanoindentation measures, Constantinides & Ulm elaborated a two-step homogenization procedure for hcp with application of the Mori-Tanaka approximation scheme. The Young modulus for both sound and leached CEM I hcp showed a good agreement with experimental results. Dormieux et al. (2007) used also a two scale model to evaluate the increase of elastic properties of a cement paste during hydration. The model refers to two types of C-S-H, the inner product constitutes layers surrounding the anhydrous particles, while the outer one plays the role of a porous matrix.

In this study the micromechanical model proposed is inspired by the one adopted by Bary & Béjaoui (2005) for the estimation of the diffusive properties of a hcp. This model relies on the assumption that the initial cement grain hydrates to form successively an external (outer) layer and an internal (inner) layer, with the aspect of a doubly coated sphere (Fig. 1). The core constituted by the unhydrated clinker corresponds to the portion of cement that has not reacted with water. Indeed, depending on the particle size distribution of the anhydrous cement and w/c some unhydrated clinker may remain in the system. This previous description is the second step of the two-scale representation of the microstructure of hcp. At the first step, the other hydrates, CH and aluminates phases are considered as spheroidal inclusions of various aspect ratios in the two types C-S-H matrix.

The first inner layer results from higher confinement conditions and from poorer accessibility during

hydration process and then is less porous than the outer one. The gel pores are then assumed to be embedded in both layers while the capillary porosity is only in the outer one. The elastic properties and the volume fractions of the different phases are taken from Stora et al. (2007). The first step composite sphere representation is similar to the well known three phase model introduced by Christensen & Lo (1986) and the effective properties are estimated by the self-consistent-scheme (Hervé & Zaoui 1993). The second step matrix-inclusions model is computed by Zheng & Du (2001) model, termed Interaction Direct Derivative scheme (IDD). The schematic representation of the two steps of the description of hcp is represented on figure 1. The input values of the volume fraction of each phase and their Young modulus and Poisson ratio are given in Table 1.

3 LAYERS BIOT COEFFICIENT

Once we made this description of hcp we propose in this section to evaluate its Biot coefficient evolution as a function of the saturation degree. The methodology is to determine the Biot coefficient of each layer (level 1) and then the macroscopic coefficient of the whole assembly (level 2). The Biot coefficient introduced by Maurice Biot (1955) represents one of the main hydro-mechanical coupling parameter in the context of THM studies. Assuming the classical Biot poroelasticity theory readapted to the case of unsaturated media, we determine the Biot coefficient of the intact material by means of the IDD and generalized self-consistent schemes.

3.1 Biot poroelasticity theory

Each layer is assumed to be homogeneous isotropic linear porous elastic medium in unsaturated conditions. Pores are regarded as spheroidal voids subjected to the stress generated by water and gas pressure. Macroscopically, the stress tensor is expressed as (Coussy 1995):

$$\sigma = 2\mu J : \varepsilon + 3kL : \varepsilon - b1p_c - 3\alpha k\theta 1 \quad (1)$$

where b is the Biot coefficient expressing the hydro-mechanical coupling and p_c the capillary pressure, ε is the macroscopic strain tensor of the representative elementary volume and $\theta = T - T_0$ with T and T_0 the current and initial temperatures, respectively; α is the coefficient of thermal expansion, μ and k are the shear and bulk moduli in isothermal drained conditions; J and K are the hydrostatic and deviatoric parts of the fourth identity tensor and 1 is the second identity tensor.

Table 1. Elastic properties and volume fractions of hcp phases.

Phases	Volume fractions	Elastic properties	
		E(MPa)	ν
Inner CSH	28.8	29.4	0.24
Outer CSH	21.6	21.7	0.24
CH	15.1	42.3	0.324
Aft, AFm	14.5	22.4	0.25
		42.3	0.325
Porosity	15.9	0.0	0.0
Anhydrous core	4.30	117.6	0.314

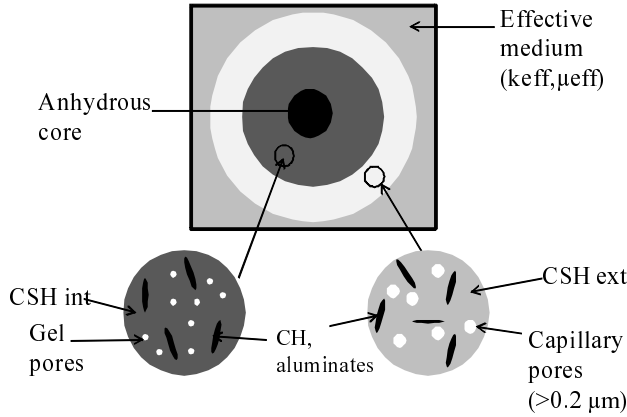


Figure 1. Schematic description of hcp microstructure. Level 1: matrix-inclusions type representation for C-S-H coating; Level 2: Three-phase assembly for hcp.

In isothermal conditions with no homogeneous macroscopic strain, the macroscopic stress becomes:

$$\sigma = -bp_c l \quad (2)$$

According to the Levin theorem, the macroscopic stress σ generated by any microscopic homogeneous eigenstress (or strain-free stresses) $-p1$ acting in the pores inclusion family is:

$$\sigma = -\langle {}^T A : p1 \rangle = -\phi \langle {}^T A : p1 \rangle \quad (3)$$

where A is the isotropic strain localization tensor, ϕ is the porosity and $\langle \cdot \rangle$ denotes the volume average operations over the pores volume and p the pressure which is exerted on the solid phase surface in the pores. By identifying both equations, the Biot coefficient is totally determined by the knowledge of the strain localization tensor A and the pressure really exerted on the solid surface:

$$b = {}^T A : 1 : 1 \frac{\langle p \rangle}{p_c} \quad (4)$$

To determine this pore pressure we assume that at a given saturation degree, we distinguish two pores families in the system: the first family is the one having radius lower than the capillary radius and totally saturated of water. The pressure exerted in

those pores is the capillary pressure due to the effects of the liquid gas interfacial tensions. In the second pores family, the liquid phase is adsorbed on the solid skeleton in the form of a thin film and is subjected to the disjoining pressure.

The latter is an equilibrium characteristic of thin films and is well known to grow up when the saturation degree approaches to zero. Furthermore its effects become non negligible if the pores are small enough to make an interaction between the liquid-solid and liquid-gas interfaces. According to Derjaguin mechanical definition (Derjaguin & Churaev 1977), the disjoining pressure Π is a change in applied external pressure p^β while passing from thick to thin planar films:

$$p^\beta = \Pi + p^\alpha \quad (5)$$

where p^α is the pressure in equilibrium bulk mother phase of thin film.

In our present case the thin film has a spherical form and we apply the recent works of A.I. Rusanov (2005) on the equilibrium thin liquid films to estimate the applied pressure p^β :

$$p_l - p_g = (p^\beta - p_l) \frac{R_n^2}{R_0^2} - \frac{2\sigma_{gl}}{R_0} \quad (6)$$

where p_l et p_g are the liquid and gas pressure, R_n is the pore radius and $R_0 = R_n - t/2$.

The influence of the disjoining pressure on the Biot coefficient as a function of the saturation degree is plotted on figure 2 for 20% of porosity. We retained a Schultz size distribution function for the porosity which permits to obtain a realistic curve of the capillary pressure as a function of the saturation degree. On figure 2, as expected the influence of the disjoining pressure is more significant at low saturation degrees. In fact at low saturation degrees the pores are mainly empty with the thin film adsorbed on the solid skeleton and subjected to the disjoining pressure whereas at high saturation degree ($S_l > 0.7$), the pores are almost full of free water.

The effect of temperature on both curves could be a further investigation of this study.

In the following paragraph we detail the determination of the strain localization tensor A .

3.2 Localization: IDD scheme

Before a detailed presentation of IDD effective approximation scheme we briefly recall in this section the general principles of homogenization theory in linear elasticity. The homogenization theory aims at estimating the effective properties of a heterogeneous material.

The first step of these methods consists in the characterization and the definition of a representative elementary volume (REV) according to two conditions: it must be large enough to be able to reproduce the heterogeneity of the microstructure and small enough compared to the size of the structure.

Let us designate by Ω the REV composed of a matrix phase labeled by 0 (in our case the inner and the outer layers) and p particulates phases indexed by i as inclusions (in our case aluminates Aft and AFm, CH, pores).

The REV is subjected to uniform strain boundary conditions at infinity

$$\xi(z) = E \cdot z \quad (7)$$

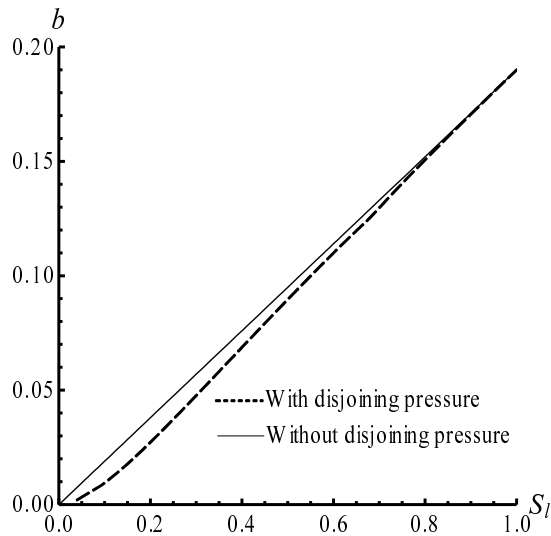


Figure 2. Influence of disjoining pressure on evolution of intact material Biot coefficient as a function of saturation degree ($\Phi = 20\%$).

where E denotes the macroscopic strain field prescribed on the REV, ξ is the corresponding displacement. The macroscopic strain E is related to the microscopic strains over the domain Ω by the following average rule:

$$\langle \varepsilon \rangle_{\Omega} = E \quad (8)$$

Assuming a linear elasticity for each phase within Ω the Hooke constitutive law is written in the following manner:

$$\sigma(z) = C(z) : \varepsilon(z). \quad (9)$$

Accordingly, to relate the microscopic strain ε to the macroscopic one E , the fourth-order localization tensor is introduced in the classical form:

$$\varepsilon(z) = A(z) : E(z) \quad (10)$$

Recalling the volumetric average rule used previously, we have $\langle A(z) \rangle_{\Omega} = I$. Taking the average stress

of the microscopic stress $\sigma(z)$ and using equation 7 the macroscopic elastic behavior is expressed in the form: $\Sigma = C^{\text{hom}} : E$ where the homogenized stiffness tensor is :

$$C^{\text{hom}} = \langle C(z) : A(z) \rangle_{\Omega} \quad (11)$$

Assuming a constant localization tensor for each phase according to the Eshelby solution of inhomogeneous inclusion, the homogenized stiffness tensor reads:

$$C^{\text{hom}} = C_0 + \sum_{i=1}^p \phi_i C_i : A_i \quad (12)$$

with ϕ_i and C_i being the volume fraction and stiffness tensor of phase i , respectively. Equation 10 shows the importance of the strain localization tensor in the accuracy of micromechanical models. The dilute scheme introduced by Eshelby relies on the basic solution of an ellipsoidal inclusion embedded in an infinite matrix. This scheme is thus not accurate for high inclusion concentrations and doesn't account for inclusion interactions. To overcome these limitations several models have been conceived. One of the most prominent models is the Mori-Tanaka (MT) standard scheme characterized by simple derivations. In this study we choose to apply the Zheng & Du scheme (IDD). This scheme is well adapted for cementitious material morphology of the matrix-inclusions type and account for spatial distributions of inclusions independently of their shape, contrary to the MT scheme. It also has the advantage to be explicit, simple and does not violate the Hashin & Shtrikmann bounds contrarily to the MT scheme in certain configurations (Torquato, 2001). The mechanical parameters obtained by IDD models results from:

$$H^{\text{IDD}} = \left[I - \sum_i H_i^d \Omega_{Di}^0 \right]^{-1} H^d \quad (13)$$

where $H = S - S_0$ and $H_i = S_i - S_0$ designate the compliance and compliance fluctuations, respectively with S_i , S_0 and S being the compliance tensors of phase i , matrix and effective medium, respectively. H^d and H_i^d are defined as the dilute estimate for the compliance increment of the effective medium and type- i inclusion. They are expressed in the following manner:

$$H^d = \sum_i H_i^d \quad \text{and} \quad H_i^d = \phi_i \left(H_i^{-1} + \Omega_i^0 \right)^{-1} \quad (14)$$

where $\Omega_i^d = C_0 (I - \Sigma_i^d)$ is called the eigenstiffness tensor according to the Eshelby problem (the super-

script d implies distribution). Σ^d_i denotes the Eshelby tensor of the inclusion-matrix cell w^{D_i} which is the union of the inclusion w_i and its surrounding matrix. The geometry of the cell and the relative position of the inclusion w_i in w^{D_i} is representative of the inclusions spatial distribution.

In the case of voids (porosity) we have:

$$H_v^d = \phi_v (\Omega_v^0)^{-1} = \phi_v C_0^{-1} (I - \Sigma_i^0)^{-1} = \phi_v C_0^{-1} T_v^0 \quad (15)$$

where T_v^0 designates the dilute polarization tensor of the void inclusion.

Note that in the case of randomly distributed inclusions, as is the case of aluminates, CH and pores in the matrix, all summed quantities in equations 11 and 12 are replaced by their average counterparts ie $H^d_i \Omega^0_{D_i}$ and Ω^0_i become $\{H^d_i \Omega^0_{D_i}\}$ and $\{\Omega^0_i\}$ respectively, the curly brackets designating the average operation over all possible orientations. For further details reader is invited to refer to Zheng & Du (2005).

The IDD strain concentration tensor of type- i family inclusions takes the form (Bary et al. 2008)

$$A_i^{IDD} = T_i^0 \left(I - \sum_j \phi_j T_j^0 (I - C_0^{-1} \Omega_{D_j}^0) C_0^{-1} (C_j - C_0) \right)^{-1} \quad (16)$$

with T_i^0 the dilute estimate of the strain localization tensor of inclusion i embedded in the matrix.

Here the aluminates, CH and pores are assumed randomly distributed in the inner and the outer layers such that the layers remain isotropic. The strain localization tensor can be decomposed into two parts, a hydrostatic and a deviatoric one:

$$A_i^{IDD} = \frac{T_i^h}{1 + \sum_j \phi_j \left[T_j^h \left(1 - \frac{k_j}{k_0} \right) - \Xi_j^h \right]} J + \frac{T_i^d}{1 + \sum_j \phi_j \left[T_j^d \left(1 - \frac{\mu_j}{\mu_0} \right) - \Xi_j^d \right]} K \quad (17)$$

with $j \in \{Aft, AFm, CH, \text{pores}\}$, Ξ_j^h and Ξ_j^d the hydrostatic and deviatoric parts of the tensor Ξ expressed as follow:

$$\Xi_j^0 = \left\{ T_j^0 (T_{D_j}^0)^{-1} \right\}. \quad (18)$$

$\Xi_j^h = \Xi_j^d = I$ when the j -type inclusions and their surrounding cell as defined previously are identical in both shape and orientation and the IDD model become analogous to the MT scheme (Bary et al. 2008).

The Biot coefficient estimation is easily obtained:

$$b = \frac{T_i^h}{1 + \sum_j \phi_j \left[T_j^h \left(1 - \frac{k_j}{k_0} \right) - \Xi_j^h \right]} \frac{\langle p \rangle}{P_c} \quad (19)$$

We propose to illustrate the theoretical IDD scheme through a simple application concerning the effect of the spatial distribution of rigid inclusions reinforcing a matrix phase. The inclusions are spherical and embedded in the matrix with spheroidal distribution (β = aspect ratio of the distribution cell). Note that the direction (1) coincides with the revolution axis of the distribution cell and direction (2) coincides with its semi-minor axis. The results of the enhancement of the axial shear modulus defined as $a = E_{11} / 2(I + \nu_{12})$, the transverse shear modulus μ_1 , and the longitudinal shear modulus μ_3 are plotted on figure 3 for 20% of inclusion volume fraction.

The Young modulus and Poisson ratio of the inclusions (E_i, ν_i) and the matrix phase (E_m, ν_m) are:

$$E_i = 2.5 E_m = 500 MPa; \nu_i = \nu_m = 0.25.$$

As expected the transverse shear modulus decrease since the rigid particles are further apart in the plane perpendicular to the axis of symmetry (Ponte Castaneda & Willis 1995).

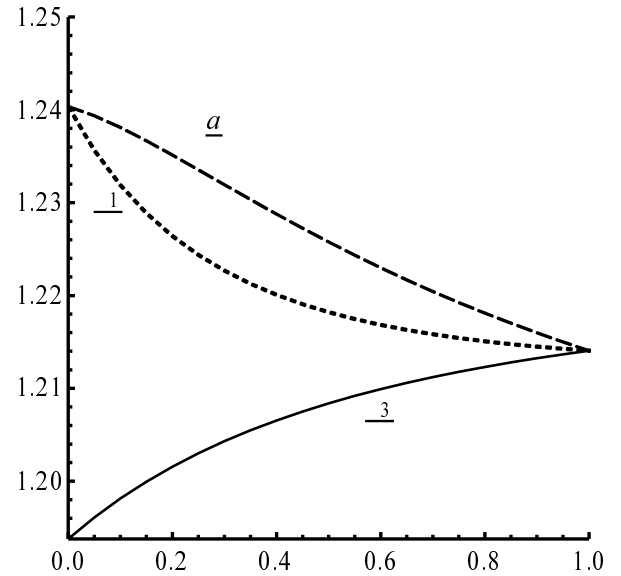


Figure 3. Estimates for the axial shear modulus, the longitudinal shear modulus and the transversal shear modulus of composite with 20% of rigid spherical inclusions.

4 BIOT COEFFICIENT OF THE WHOLE ASSEMBLY (INTACT MATERIAL)

In this section we refer to the procedure used by Bary & Béjaoui (2005) for determining the effective diffusion coefficient of hcp regarded as multi-coated sphere assemblage. This procedure relies on the condition that a sphere inserted into an infinite homogeneous medium obeys the equation 20 and does not provoke any perturbation in the body fields. The phases are considered as homogeneous and isotropic linear elastic porous media. The local stress-strain is defined by:

$$\sigma = 2\mu J : E + 3kL : E - bpI \quad (P) \quad (20)$$

This problem P is viewed as the superposition of two distinct loading conditions, the macroscopic strain and the internal pressure p: (E = 0; p)≡P' and (E = p; 0)≡P''. The total stress and strain are then obtained by summing their counterparts for both problems P' and P''. By means of Hervé & Zaoui (1993) (n+1)-layered sphere model, the problem P'' permits to determine the macroscopic bulk modulus k_{eff} . The expression of k_{eff} for two-phase sphere is:

$$k_{eff} = k_2 + \frac{(3k_2 + 4\mu_2)(k_1 - k_2)\phi}{4\mu_2 + 3k_1\phi_2 + 3k_2\phi_1} \quad (21)$$

The Problem P' is completely determined with the following classical conditions for displacement and traction at the boundary surfaces core-shell (radius R_1) and shell body:

$$u_1(0) \text{ Finite; } u_1(R_1) = u_2(R_1)$$

$$\Sigma_1(R_1)r = \Sigma_2(R_2)r, \quad u_2(R_2) = 0 \quad (22)$$

The continuity condition of the traction vector across the shell body interface yields an expression the effective Biot coefficient b_{eff} and the mechanical parameters of the two-phase sphere:

$$\Sigma_2(R_2)r = \Sigma(R_2)r = -b_{eff} p.r \quad (23)$$

The exact solution of equations 22 and 23 leads to:

$$b_{eff} = b_2 + \frac{(3k_2 + 4\mu_2)(b_1 - b_2)\phi}{4\mu_2 + 3k_1\phi_2 + 3k_2\phi_1} \quad (24)$$

This result corresponds to the well known formula of Levin (1967) giving the overall thermal expansion coefficient α_{eff} providing the introduction of k_{eff} in equation 24 and the replacement of b_{ip} by $-3k_i\alpha_i\theta$ in the local stress strain relation and b_{eff} by $-3k_{eff}\alpha_{eff}$ in equation 20 for the thermoelastic behavior; θ is the variation of temperature from initial conditions.

Equation 24 shows that only the Biot coefficient and the bulk modulus of the core of the composite sphere is needed to calculate the effective Biot coefficient. b_{eff} . These two parameters could be exactly known in the case of multi-sphere coated assemblage if we refer to the (n+1)-layered sphere model and to the correspondence between equations 21 and 24.

In fact considering a (n+1)-phase material, the phases 1 to n are interpreted as a single phase with characteristics b_n^{eff} and k_n^{eff} which form the core of the previous two-phase model, and we obtain the overall Biot coefficient: (Bary & Béjaoui 2005)

$$b_{n+1}^{eff} = b_{n+1} + \frac{(3k_{n+1} + 4\mu_{n+1})(b_n^{eff} - b_{n+1})(1 - \xi_{n+1})}{4\mu_{n+1} + 3k_n^{eff}\xi_{n+1} + 3k_{n+1}(1 - \xi_{n+1})} \quad (25)$$

$$\xi_{n+1} = \phi_{n+1} \left(\sum_j^{n+1} \phi_j \right)^{-1} \quad (26)$$

In our particular three phase sphere model the expression of Biot coefficient involving only the elementary phase parameters is:

$$b_3^{eff} = b_3 + \frac{(3k_3 + 4\mu_3)(1 - \phi_3)T}{9k_1k_2\phi_3(1 - \phi_3) + 12\mu_2k_1\phi_3 + (4\mu_3 + 3k_3(1 - \phi_3))(4\mu_2(1 - \phi_3) + 3k_1)} \quad (27)$$

$$T = [(b_2 - b_3)(4\mu_2(1 - \phi_3) + 3k_1) - \phi_1(b_2 - b_1)(4\mu_2 + 3k_2)]$$

with $k_{12} = k_1\Phi_1 + k_2\Phi_2$ and $k'_{12} = k_2\Phi_1 + k_1\Phi_2$

5 HYDROMECHANICAL PARAMETERS OF MICROCRACKED CONCRETE

This section deals with the determination of the Biot coefficient of the material weakened by microcracks. The influence of these latter on the effective properties of quasi-brittle materials like concrete has been investigated through various phenomenological models (e.g., Lemaitre & Chaboche 1992). However some concepts used to describe the failure process do not rely on physical observations at microscopic scale. An alternative way is the micromechanical approaches based on the analysis of the microstructure of the material. We distinguish in the literature two classes of micromechanical models devoted to microcracked materials. The first one is the direct approach (Nemat-Nasser & Hori 1990, Kachanov 1982, Pensée & Kondo 2001) and is generally based on the analysis of the displacement fields discontinuity induced by microcracks. These models are usually limited to dilute distribution of microcracks and are not able to take into account the interactions between microcracks and the effects of their spatial distribution (Zhu et al. 2007). The second class corresponds to the homogenization models, which permit to overcome these limitations. The cracked material is considered as a matrix-inclusion type material and the effective properties are determined by up-scaling techniques.

Microcracks are described by penny-shaped ellipsoids classically characterized by their normal \underline{n} , main radius a and average half opening c . We call aspect ratio $\alpha = c / a$. In this study we examine the case of a material weakened by aligned self-similar penny-shaped ellipsoidal voids with a given aspect ratio α and centers distributed with ellipsoidal symmetry β . Such distributions of microcracks, which

can be observed experimentally in the case of uniaxial tension or compression loadings induces a transversely isotropic behavior of the material. We further have a non isotropic Biot tensor contrary to the classic case of randomly distribution of the microcracks.

We assume that the microcracks aspect ratios α tends to 0, consequently the tensor $(I - \Sigma^0_i)$ is singular, whereas $\alpha (I - \Sigma^0_i)$ has a finite value. The latter expression in the Walpole base is expressed as (Deudé et al. 2002):

$$T = \lim_{\alpha \rightarrow 0} \alpha (I - \Sigma^0_i) = \frac{4(1-\nu_s)}{\pi} \begin{pmatrix} 0 & \frac{1-\nu_s}{1-2\nu_s} & 0 & \frac{1}{2-\nu_s} & \frac{\nu_s}{2-\nu_s} & 0 \end{pmatrix} \quad (28)$$

The volume fraction of microcracks is:

$$\phi_c = \frac{4}{3} \pi a^2 c N = \frac{4}{3} \pi \alpha \rho \quad (29)$$

where N denotes the number of cracks per unit volume (crack density), ρ is the crack density parameter and used as internal damage variable in some micromechanical studies (e.g. Pensée & Kondo 2003, Deudé et al. 2002).

Referring to the equation 13 it seems more practical to express C^{hom} as a function of the tensor T .

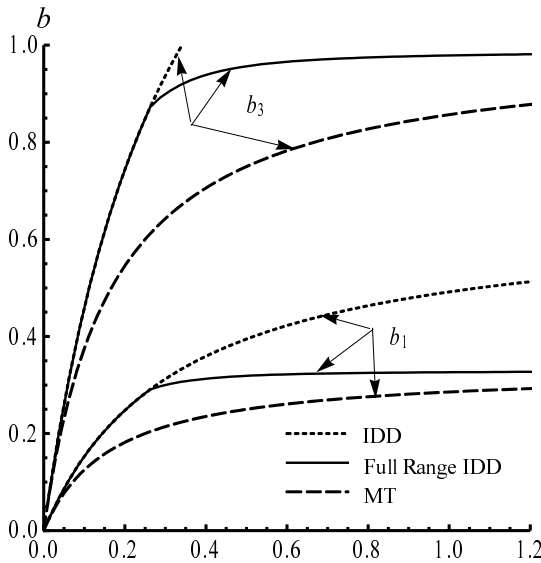


Figure 4. Evolution of the Biot tensor terms as a function of the microcrack density parameter (Comparison between IDD, Full Range IDD and MT models).

$$C^{hom} = C^s : \left(I + \frac{4\pi}{3} \rho T \left(I - \frac{4\pi}{3} \rho T S^s \right)^{-1} \right)^{-1} \quad (30)$$

The Biot tensor of the weakened material is expressed as (Dormieux et al. 2006):

$$B = 1(I - S^s : C^{hom}) \quad (31)$$

where S^s is the compliance tensor of the solid phase and C^{hom} the effective stiffness tensor of the homogenized medium. According to the transversely isotropic behavior of the medium the Biot tensor can be expressed as:

$$B = b_1 (e_1 \otimes e_1 + e_2 \otimes e_2) + b_3 e_3 \otimes e_3 \quad (32)$$

where e_3 is the direction normal to the microcracks.

Explicit results are obtained for a flat distribution of microcracks ($\beta = 0$) which is equivalent to the MT scheme:

$$b_1 = \frac{4d(1-\nu_s)\nu_s}{\pi + 4d(\nu_s - 1)^2 - 2\pi\nu_s} \quad (33)$$

$$b_3 = b_1 \frac{1-\nu_s}{\nu_s} \quad (34)$$

where $d = 4\pi\rho/3$.

The evolutions of the Biot tensor terms b_1 , b_3 in the case of aligned microcracks, as a function of the microcracks density parameter ρ are plotted on figure 4 for different schemes ($\beta = 1$ in the case of IDD scheme). Note that for a given aspect ratio of the penny-shaped ellipsoids α , and for consistency with the hypothesis of impenetrability of the inclusions cells, one has a maximum value of microcracks porosity Φ_{max} . This value represents a physical bound for the IDD scheme in the case of isotropic distribution. To be able to take into account higher inclusions concentration Zheng & Du (2005) have proposed to adopt ellipsoidal distribution of inclusions denoted as Full Range IDD method.

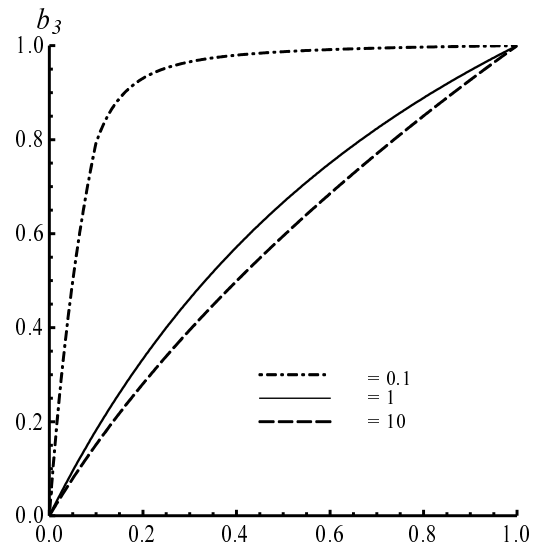


Figure 5. Effects of voids aspect ratio on the longitudinal term on the Biot tensor, Full Range IDD.

For microcracks ($\alpha = 0$), Φ_{max} is equal to $3/4\pi$ and corresponds to the point where the Full Range IDD and IDD curve diverge (Fig. 4).

We can see that the longitudinal Biot tensor in the case of Full Range IDD tends to 1 for intense cracking. We can also remark that the IDD model overestimates the longitudinal Biot tensor since it reaches the maximum value 1 for a microcrack density parameter $\rho \approx 0.35$. For intense cracking, the axial Biot tensor tends to a finite value which can be expressed as a function of the matrix mechanical parameters.

It is interesting to notice that the aligned microcracks not only affect the longitudinal bulk modulus of the material, but also the axial Biot coefficient b_1 which is significantly increased.

In order to show the influence of voids aspect ratio on the evolution of the Biot tensor, we depicted on figure 5 the evolution of the longitudinal term b_3 (calculated with Full Range IDD scheme) of the Biot tensor with three values of aspect ratio representing both oblate ($\alpha = 0.1$), spherical ($\alpha = 1$) and prolate ($\alpha = 10$) shape inclusions. We can notice that the pores with oblate shape affect more significantly the effective properties than those with prolate ones. This result is in agreement with the well known feature that at a given volume fraction, the oblates pores have more influence on the effective properties than prolates one (Torquato 2001).

6 CONCLUSION

A microstructural description of hcp as previously proposed in (Bary & Béjaoui 2005) is adopted based on the hydration process of the cement grain. The latter, assumed spherical, hydrates to form successively an external and an internal layer; these doubly-coated spheres fill all space so that the resulting assemblage is equivalent to the three-phase sphere model. This description of hcp involves the main hydrates of the cement paste. The Biot coefficient of each layer of the doubly-coated sphere is then determined by means of the IDD model. The influence of the disjoining pressure arising in the water layers adsorbed on desaturated pore surfaces on the Biot evolution as function of the saturation degree is investigated.

In this paper, microcracks are represented by penny-shaped voids. Aligned microcracks are considered such that the resulting effective medium is transversely isotropic. We then investigate the influence of spatial distribution of microcracks and shape of void inclusions on hydromechanical effective properties.

Results show that closed microcracks affect significantly the Biot tensor and as expected the longitudinal Biot coefficient is greater than the axial Biot coefficient. Full Range IDD is applied to account for high inclusion concentration and permit to give more physical sense to results. A further development of this work could be the extension of the re-

sults in the framework of a thermo-hydro-mechanical study. The influence of the frictional mechanism appearing in closed microcracks on the material effective properties could be also investigated.

REFERENCES

- Bary B., & Béjaoui S. 2005. Assessment of diffusive and mechanical properties of hardened cement paste using a multi-coated sphere assemblage model. *In Cement and Concrete Research* 36 (2006) 245-248.
- Bary B., 2008. Estimation of mechanical parameters in unsaturated microcracked concrete.
- Biot M.A., 1955. Theory of elasticity and consolidation for a porous anisotropic solid. *In Journal of Applied Physics*.
- Christensen R.M. & Lo K.H., 1979. Solutions for effective shear properties in three phase sphere and cylinder models. *In journal of Mechanics and Physics of Solids* Vol 27, pp 315-330.
- Constantinides G, & Ulm F.J., 2007. The effect of types of C-S-H on the elasticity of cement based materials: results from nanoindentation and micromechanical modeling. *In Cement and Concrete Research* 31 (1) 2004 67-80.
- Constantinides G., & Ulm F.J., 2007. The nanogranular nature of C-S-H. *In Journal of Mechanics and Physics Solids* 55 (1) 2007 -64-90.
- Coussy O., 1995. Mechanics of porous continua, John Wiley & Sons 1995.
- Derjaguin B., Churaev, N. 1977, *In Journal of Colloid Interface Science* 62, 369.
- Deudé V., 2002. Non linéarités géométriques et physiques dans les milieux poreux: Apport des changements d'échelle. *PhD Thesis, Ecole Nationale des ponts et chaussées*.
- Dormieux L., & Kondo D. & Ulm F.J., 2006. Micromechanics. Chichester, England.
- Hervé E., & Zaoui A., 1993. N-layered inclusions-based micromechanical modeling. *In International Journal of Engineering Science* 31 (1) 1993 1-10.
- Lemaître J., 1992. A course on damage mechanics, second ed. Springer, Berlin.
- Levin V.M., 1967. Thermal expansion coefficients of heterogeneous material. *In Mechanics of Solids* 21 (1967) 9-17.
- Nemat-Nasser S., Hori M., 1993. Micromechanics: Overall properties of heterogeneous materials. North Holland, The Hague Boston.
- Obeid W. & Mounajed G., 2001. Experimental identification of Biot' hydro-mechanical coupling coefficient for cement mortar. *In Materials and structures, Vol.35, May 2002, pp 229-236*.
- Pensée V. & Kondo D., 2003. Micromechanics of anisotropic brittle damage: comparative analysis between a stress based and a strain based formulation. *In Journal of Engineering Mechanics ASCE*, 128.
- Ponte-Castaneda P., & Willis J.R., 1995. The effect of spatial distribution on the effective behavior of composite material and cracked media. *In Journal of Mechanics and Physics Solids* 43 (12) 1995 1919-1951.
- Sanahuja J., Dormieux L., Chanvillard G., 2007. Modelling elasticity of a hydrating cement paste. *In Cement and Concrete Research* 37 (10) 2007 1427-1439.
- Stora E., Bary B., He Q.C., 2006. On estimating transport properties of hardened cement paste.. *In Cement and Concrete Research* 36(7) 2006 1330-1344
- Stora E., 2007. Multi-scale modeling and simulations of the chemo-mechanical behavior of degraded materials *PhD Thesis, Université Marne la vallée*

- Torquato S., 2001. *Random Heterogeneous Materials*, Springer, New York.
- Zheng Q.S., & Du D.X.. 1993. An explicit and universally applicable estimate for the effective properties of multiphase composites which accounts for inclusion distribution. *In Journal of Mechanics and Physics Solids* 49 (11) 2001 2765-2788.
- Zhu Q.Z. & Kondo D., 2007. Micromechanical analysis of coupling between anisotropic damage in quasi-brittle materials: Role of homogenization scheme. *In International Journal of Solid and Structures* 45 (2008) 1385 1405.